Posture similarity index: A method to compare hand postures in synergy space

Nayan Bhatt [1] , **Varadhan SKM** [Corresp. 1]

[1] Department of Applied Mechanics, Indian Institute of Technology Madras, Chennai, India

Corresponding Author: Varadhan SKM
Email address: skm@iitm.ac.in

Background

The Human hand can perform a range of manipulation tasks, from holding a pen to holding a hammer. Central Nervous System (CNS) uses different strategies in different manipulation tasks based on task requirements. Attempts to compare postures of the hand have been made, for use in robotics and animation industries. In this study, we developed an index called the posture similarity index, to quantify the similarity between two human hand postures.

Methods

Twelve right-handed volunteers performed 70 postures, and lifted and held 30 objects (total of 100 different postures, each performed five times). A 16-sensor electromagnetic tracking system captured the kinematics of individual finger phalanges (segments). We modeled the hand as a 21-DoF system and computed the corresponding joint angles. We used principal component analysis to extract kinematic synergies from this 21-DoF data. We developed a posture similarity index (PSI), that represents the similarity between posture in the synergy (Principal component) space. First, we tested the performance of this index using a synthetic dataset. After confirming that it performs well with the synthetic dataset, we used it to analyze the experimental data. Further, we used PSI to identify postures that are "representative" in the sense that they have a greater overlap (in synergy space) with a large number of postures.

Results

Our results confirmed that PSI is a relatively accurate index of similarity in synergy space both with synthetic data and real experimental data. Also, more special postures than common postures were found among "representative" postures.

Conclusion

We developed an index for comparing posture similarity in synergy space and demonstrated its utility by using synthetic dataset and experimental dataset. Besides, we found that "special" postures are actually "special" in the sense that there are more of them in the "representative" postures as identified by our posture similarity index.

1 **Posture similarity index: A method to compare hand**

2 **postures in synergy space**

3 Nayan Bhatt[1], Varadhan SKM[1]

4 [1] Department of Applied Mechanics, Indian Institute of Technology Madras, Chennai, Tamil

5 Nadu, India

6 Corresponding Author:

7 Varadhan SKM [1]

8 Department of Applied Mechanics, Indian Institute of Technology Madras, Chennai, Tamil

9 Nadu, India

10 Email address: skm@iitm.ac.in

Abstract

Background

The Human hand can perform a range of manipulation tasks, from holding a pen to holding a hammer. Central Nervous System (CNS) uses different strategies in different manipulation tasks based on task requirements. Attempts to compare postures of the hand have been made, for use in robotics and animation industries. In this study, we developed an index called the posture similarity index, to quantify the similarity between two human hand postures.

Methods

Twelve right-handed volunteers performed 70 postures, and lifted and held 30 objects (total of 100 different postures, each performed five times). A 16-sensor electromagnetic tracking system captured the kinematics of individual finger phalanges (segments). We modeled the hand as a 21-DoF system and computed the corresponding joint angles. We used principal component analysis to extract kinematic synergies from this 21-DoF data. We developed a posture similarity index (PSI), that represents the similarity between posture in the synergy (Principal component) space. First, we tested the performance of this index using a synthetic dataset. After confirming that it performs well with the synthetic dataset, we used it to analyze the experimental data. Further, we used PSI to identify postures that are "representative" in the sense that they have a greater overlap (in synergy space) with a large number of postures.

Results

Our results confirmed that PSI is a relatively accurate index of similarity in synergy space both with synthetic data and real experimental data. Also, more special postures than common postures were found among "representative" postures.

Conclusion

We developed an index for comparing posture similarity in synergy space and demonstrated its utility by using synthetic dataset and experimental dataset. Besides, we

52   found that "special" postures are actually "special" in the sense that there are more of them

53   in the "representative" postures as identified by our posture similarity index.

Introduction

55 Accurate modeling of hand and finger postures is of interest in robotics and animation industry. In

56 the animation industry, differentiation of one hand posture from another is crucial for the

57 perception of a gesture and to bring in a more "lifelike" appearance (Hoyet et al 2012). In robotics,

58 the comparison of a robotic posture with the biological (human) hand posture is useful to assess

59 the performance of a robot (Feix et al 2013).

60

61 Studies in perception of animations have exploited the relatively low number of dimensions that

62 are required to distinguish between perceived postures (Hoyet et al 2012). So they used a relatively

63 small number of markers to produce postures that are perceived as different. Studies in robotics

64 have focused on the development of methods to compare a robotic posture with hand posture, the

65 "anthropomorphism index" (Feix et al 2013, Romero et al 2010). Other works have focused on

66 exploring the low-dimensional subspace used by human hand postures (Ciocarlie & Allen, 2009,

67 Wheatland et al 2013). These studies are performed in line with the hope that understanding human

68 grasping could improve the design of grasping robots. These approaches attempt to compare

69 human hand postures with those generated by a computer (animations) or by a robot (robotics).

70 These studies have not attempted a comparison of a human hand posture with another human hand

71 posture.

72 In the field of motor control, several studies have attempted to characterize and model hand

73 postures (Santello 1998; Gentner & Classen, 2006; Cavallo et al., 2016; Leo et al 2016). Many of

74 these studies have used Principal Component Analysis (PCA) to identify the dominant dimensions

75 in the multi-dimensional space of a set of hand and finger postures (where a set of joint angles is

76 used to quantify each posture). Many of these studies quantified and presented the proportion of

77 variance explained by these dominant dimensions.

78 However, these studies have not attempted comparison of postures per se. As such, assessment of

79 similarity is a challenging problem. Some relatively sophisticated algorithms have been proposed

80 (e.g. Roweis & Saul, 2000) to assess similarity. We believe that a method to specifically compare

81 human hand postures in synergy space would be useful in the field of motor control, animation,

82 and robotics. We attempt to develop such a method in this paper.

83 In this study, we propose, define, and develop an index (posture similarity index, PSI), that

84 quantifies similarity in the principal component ("synergy") space. We first test this index on a

85 synthetic dataset and then with a small experimental dataset. We then use this index to study

86 similarity across a large number of postures (100 postures, including both everyday life and special

87 postures). Based on PSI, we identify representative postures that may reflect dimensionality of

88 hand action in the synergy space. These representative postures are those that have a relatively

89 large overlap in synergy space with several postures. Among this set of "representative postures",

90 we further compare the number of everyday life postures and "special" postures.

91 **Materials & Methods**

92 **Participants**

93 Twelve right-handed volunteers (six males and six females [Age: 25.5 ± 1.55 (SD) years] provided

94 written informed consent and participated in the study. No participant had a history of any

95 neurological disorder or any trauma to the upper extremity. All experimental procedures were

96 approved by the Institutional Ethics Committee of IIT Madras (Approval number:

97 IEC/2016/02/VSK-1/11). All participants were naive to the purpose of the study.

98 **Experimental procedure**

99 The experimental procedure involved performing simple motor acts including specific hand

100 postures and object manipulation. For the collection of kinematic information, we used

101 electromagnetic tracking sensors (Diameter 1.8mm, Resolution 1.27 microns, Static position

102 accuracy 0.76mm, Static angular orientation accuracy 0.15 degree, Polhemus Inc., USA, Model:

103 Liberty micro sensors). For preventing interference, we minimized the number of metallic objects

104 in the experimental room. We placed the sensors on the dorsal side of digits (I: Index; M: Middle;

105 R: Ring; L: Little) using double sided adhesive tape as shown in Figure 1 (A). These sensors

106 captured the movement of distal segment/phalanx, middle segment/phalanx, proximal

107 segment/phalanx, and metacarpals. From these quantities, we derived the distal interphalangeal

108 (DIP), proximal interphalangeal (PIP), and metacarpophalangeal (MCPs) joint angles for I, M, R,

109 and L. For the thumb, we measured the movements of distal, proximal, and metacarpal segments

110 and we computed the interphalangeal (IP), metacarpophalangeal (MCP), and carpometacarpal

111 (CMC) joint angles. We mounted the reference sensor near proximal part of the wrist between 2nd

112 and 3rd metacarpal bone. We designed a customized user interface in LabVIEW (National

113 Instruments) environment to collect data at 120 Hz, and performed offline analysis using

114 MATLAB (MathWorks, USA).

115 (Figure 1)

116 **Kinematic data acquisition**

117 The experimental setup is presented in Figure 2. Placement of sensors in the lab coordinate system

118 was designed according to biomechanical standards (Wu et al., 2005). We defined a base posture

119 at the start of every trial. In this base posture, the hand is in pronation position with all the fingers

120 (including the thumb) fully extended and adducted. Participants were seated in a height adjustable

121 chair comfortably with his/her arm resting on the table at approximately wrist level, with palm

122 facing the surface of the table. A 24-inch LED monitor was placed approximately 1 meter away

123 from the participants.

124 (Figure 2)

125 The experiment consisted of two types of tasks. The first type of task called the externally

126 constrained postures included 30 postures that involved manipulation of an object. The second

127 type of task called the internally constrained postures, included 70 free hand postures that did not

128 involve object manipulation, hence constrained only by the CNS. The participants viewed pictures

129 of target postures for internally constrained postures (i.e. American Sign Language (ASL), Indian

130 dance form Bharatanatyam) on a computer screen. At the beginning of each trial, the participant

131 started from the base posture and reached the target posture. Each trial was five seconds long, and

132 was repeated five times. Hence, participants performed a total of 500 (100 postures x 5 trials per

133 posture) trials. There was a rest period of ten seconds between trials. Additional rest was provided

134 during the experiment whenever the participant requested.

135 For the externally constrained postures, before each trial, an object was placed on a predefined

136 marked position, nearly 15 cm away from the hand. Participants were then asked to lift and hold

137 the object approximately 10 cm above the surface. The experimenter visually compared the static

138 posture at the end of the trial with the target posture. The experimenter also carefully observed all

139 the trials and repeated any trial in which the posture was not faithfully performed. On an average,

140 less than 2% of the trials were repeated across participants. We have presented the set of all the
141 postures in the Supplementary material.

Data processing and kinematic model

143 We computed all joint angles using the principles of mechanics (Zatsiorsky 1998; Jazar 2010). We
144 considered the trial duration from ~3.6 to 4.25 seconds as static posture (i.e. 70 samples) because
145 the change in joint angles were not significant after 3.6 seconds across postures and we dropped
146 the last few samples to avoid the end of the trial effects. Joint angle data was filtered using second-
147 ordered zero-lag low pass Butterworth filter. For removing any possible effect of physiological
148 tremors in static postures, we set the cutoff frequency at 4.5Hz. The frequency content of these
149 tremors has been reported to be in multiple ranges of frequencies (Deuschl et al 2001; Fahn et al
150 2011; McAuley et al 2000). The general agreement between these studies is that tremor frequencies
151 are below 5 Hz, although maximum frequencies vary. Our goal was to compare static postures (not
152 movements); hence we chose a low value of cutoff frequency. We constructed a matrix of size
153 35,000 (5 trials x 100 postures x 70 samples per posture) x 21 (dimension) from the entire data for
154 each participant, and used this matrix for further analysis.

155 The hand model had 21 degrees of freedom (DoF) as shown in Figure 1 (B) (similar to Rezzoug
156 et al., 2008). In this model, each finger was considered to have four DoFs: it included flexion-
157 extension (Flex-Ext) of DIP and PIP joints; it also included flexion-extension and abduction-
158 adduction of MCP joint. We represented the thumb with five DoFs which included flexion-
159 extension of IP and MCP joint, and three DoFs which included flexion-extension, abduction-
160 adduction, and axial rotation from CMC joint.

Exploring kinematic synergy space using a linear method

162 There is a strong relationship between DIP and PIP joint angles for I, M, R, and L. DIP Vs PIP
163 joints across twelve participants showed a linear relationship (r^2=0.997) between these joints
164 across fingers. Dependency and amount of co-dependency may vary. However, covariation
165 patterns are stereotypical. For quantification of variance explained by PCs, we used Principal
166 Component Analysis (PCA). Static hand postures were transformed from joint angle space to space
167 with basis vectors orthogonal to each other (i.e. "synergy space") using the PCA method. The
168 dataset (35000 samples = 5 trials x 100 postures x 70 samples per posture) were analyzed.
169 Dimensionality of the dataset is 21 considering 21 DoFs hand model. We performed PCA by

170   centering the data and using Singular Value Decomposition (SVD) algorithm. Variance explained

171   by principal components in synergy space are plotted across participants.

172

173

174

175

176   **Posture Similarity Index (PSI)**

177   Comparing two different hand postures in the synergy space, rather than in joint angle space, may

178   provide insightful information about overlap (in synergy components) between two postures. The

179   measure developed by us compares two hand postures in synergy space and gives a quantification

180   number called Posture Similarity Index (PSI).

181   **Theoretical formulation**

182   Joint angle space spanned by various hand movements is also termed as *action manifold* (Feix et

183   al., 2013). Our objective is to find a subset of postures that may help in exploring 21-dimensional

184   space in the best possible way. We also included a set of extreme postures in the study to explore

185   individual degrees of freedom of hand. One approach to study hand postures in synergy subspace

186   is dimensionality reduction (Santello et al 1998). An alternative view is that the control signal

187   helps controlling multiple degrees of freedom simultaneously (Todorov, 2002; Todorov et al.,

188   2004). In synergy space, some postures might be similar to others. Due to such similarity between

189   postures, it is possible to derive one posture by minor modification in synergies of a slightly

190   different posture. However, if two postures are very different, it is not expected that minor

191   modification of synergy of one posture will lead to the other posture. Quantifying the similarity

192   between postures will help us find the representative postures. For each participant, the dataset

193   contained 100 static hand postures and 35000 (5 trials x 100 postures x 70 samples per posture)

194   samples with 21 dimensions. Since there is no learning or history effect between trials of a posture,

195   we selected a random trial from five trials for every posture separately, resulting in 100 selected

196   trials per participant (one trial per posture). We assumed that any one of the five trials is

197   representative of the 5 trials performed. Note, however, that the "average" of the five trials may

198   not represent each individual trial. We used PCA to project static hand postures from joint angle

199   space to synergy space. Before applying PCA, we performed column-wise normalization for all

200   joint angles.

201   Let the original dimensions of the data space be D (in this case dimensionality is 21, refer to Figure

202   1 (B)). Projection matrix (W, dimension NxN) was created using all static posture samples (35000)

203   that transformed static posture from joint angle space to multidimensional synergy space. All static

204   postures were projected along eigenvectors separately using projection matrix (W) giving

205   projected values (70xN). Note that in our case, static posture has dimensions of 70x21 (70 data

206   points and 21 joint angles).

207   The covariance matrices ($\Sigma(i)$, dimension NxN (i.e. 21x21); for i=1 to 100) were computed from

208   projected postures in feature space for each posture (70xN) separately. Diagonal elements of Σ

209   represent the amount of variance in each PC direction. Variances (σ^2) are expected to be similar

210   for similar postures. The ratio of variances (*i.e.* $F=\sigma^2_{1,1}/\sigma^2_{1,2}$) for two similar postures will be

211   closer to 1. If postures are not same, the weighted ratio (i.e. λF) will give two different values. To

212   avoid mathematical ambiguity, we always chose *F* less than one in all cases.

213   Based on eigenvalues (λ) of PCs, weights were assigned to *F* ratio. For generating *posture*

214   *similarity index (PSI),* we performed summation across all the N PCs. *PSI* is expected to be higher

215   for two similar postures in synergy subspace.

$$F_n^{i,j} = \frac{\sigma_{ni}^2}{\sigma_{nj}^2} \tag{1}$$

216

217   Where *F* is the ratio of two variances in the nth PC direction.

$$PSI(i,j) = \sum_{n=1}^{N} \lambda_n F_n^{i,j} \tag{2}$$

218

219   Where i, j represent similarity between the ith and j[th] posture. λ_n represents Eigen value of nth Eigen

220   vector. PSI is the weighted sum of all variance ratios across N dimensions.

221 **Evaluation of PSI on synthetic data**

222 To test the performance of our approach, we decided to first test the algorithm on a synthetic

223 dataset. Three synthetic postures were generated using multivariate normal distribution using the

224 following mean values and standard deviations. For posture 1 (mean ± S.D in X, Y, and Z, 5 ±

225 1.85, 2 ± 1.78, 10 ± 2.42), for posture 2 (mean ± S.D in X, Y, and Z, 10.54 ± 1.85, 7.35 ± 1.78,

226 17.25 ± 2.42). Mean for the second posture is generated using the following equation:

$$Mean\ (p2) = mean\ p1 + 3 * \sigma(p1) \qquad (3)$$

227

228 For posture 3, we used mean ± S.D in X, Y, and Z, 5.69 ± 0.694, 2.611 ± 0.61, 11.021 ± 1.02 for

229 generating data points. Mean for the third posture was near to first posture since we wanted to

230 overlap the data. Mean for the third posture is calculated using the following equation:

$$Mean\ (p3) = mean\ p1 + 1 * \sigma(p3) \qquad (4)$$

231

232 Using these, we generated synthetic postures, each containing 500 samples. The variance of

233 posture 1 and posture 2 are same which is (3.42, 3.17, 5.83), the variance of posture 3 is smaller

234 than other postures (0.48, 0.37, 1.043). Mean of posture 1 (represented in red) and posture 3

235 (represented in blue) are closer to each other and mean of posture 2 (represented in green) is far.

236 Variance of posture 1 and 2 are similar but posture 3 has smaller variance, and orientation of

237 posture 3 data is different in the space. There is an overlap between postures 1 and 3 as shown in

238 Figure 3 (A). We deliberately chose such a dataset to check if our method could capture the details

239 described above.

240 (Figure 3)

241 We normalized the data before the application of PCA. For extracting kinematic synergies from

242 the simulated dataset, we performed PCA. The 1st principal component (synergy) explains

243 approximately 77% of the variance, the 2nd principal component explains approximately 15% of

244 the variance, and the 3rd component explains approximately 6% of total variance, as illustrated in

245 Figure 3 (B).

246   We used projection matrix W (3x3) to project data (1500x3) on synergy space/global PC space.

247   We computed covariance matrices (Σ_i 3x3, for i=1:3) for the projected dataset. Diagonal elements

248   of the covariance matrix represent the projection of each posture in PC direction.

249   The projection ratio in each PC direction is computed and presented in Supplemental Table S1.

250   Each ratio ($F_n^{i,j}$), computed as given in equation (1) is multiplied with respective Eigen values (λs)

251   and finally added. We performed this exercise for all the postures and developed the posture

252   similarity matrix. Each element in the matrix represents *posture similarity index* comparing the

253   amount of similarity between the two postures.

254   The ratio is selected based on the condition that we chose F to be less than unity. The magnitude

255   of each Eigen vector is 0.062, 0.0127, and 0.0054. Elements for the *PSI* matrix are computed using

256   equation (5).

257
$$PSI_{i,j} = \sum_{n=1}^{3} \lambda_n * F_n^{i,j} \qquad\qquad (5)$$

258

259   From the matrix of posture similarity in Supplemental Table S2, we can observe that postures 1

260   and 2 are more similar in comparison to postures 1 and 3 and postures 2 and 3. Postures 1 and 2

261   have the same variance and structure with the mean shifted. However, posture 1 overlaps with

262   posture 3 which has closer mean value, but the structure of posture 1 is different from posture 3.

263   We note that this method (PSI) preserves the inherent structure of the data. PSI index is not only

264   a mere quantification of overlap of two postures in 2D space; rather it compares the similarity

265   between two postures in the multidimensional synergy space. The advantage of using synergy

266   space is that the reproduction of joint angles is relatively accurate. A significant value of PSI index

267   between two postures shows that there is a greater overlap of two postures in synergy space. If the

268   value of PSI is smaller between two postures, it means that the overlap of two postures in synergy

269   space is lesser.

270   In this example of synthetic data, the value of PSI between postures 1 and 2 is 0.0757, whereas

271   PSI between postures 1 and 3 is 0.0587. In this case postures 1 and 2 are more similar in

272   comparison to postures 1 and 3. Structure and variance (SD) of posture 3 are different from that

273   of postures 1 and 2. Hence we need more synergies for transforming from posture 1 to 3.

274   We performed normalization of PSI matrix using equation (6).

$$Normalised\ PSI_{i,j} = \frac{PSI_{i,j}}{\max(PSI_j)} \qquad (6)$$

275   Normalized PSI index gives the values for postures 1, 2, and 3 as listed in Supplemental Table S3.

276   **PSI for the experimental test dataset**

277   We computed the posture similarity index (PSI) for real experimental data. Each posture contained

278   seventy samples and 21-dimensional data. For the purpose of illustration, we randomly selected a

279   single posture with three different trials. We normalized the data before transforming from joint

280   angle space to synergy space using PCA. First synergy component explains nearly 63% of the

281   variance. Second synergy component explains roughly 23% of total variance and third synergy

282   component explains around 9% of the variance. We have presented the screen plot in Figure 4.

283   (Figure 4)

284   Kinematic synergies generated by PCA by projecting joint angles on synergy space will give 21

285   different synergy components.

286   We considered all the 21 PCs for further analysis. We used the projection matrix W (21x21) for

287   transforming from joint angle space to synergy space. We computed the covariance matrix (Σ_i for

288   i=1:21, 21x21) for individual postures in synergy space. Diagonal elements of covariance matrix

289   explain variance in each PC direction. For generating PSI index, we multiplied individual PC ratio

290   (F) with respective weights (λ) and then summed up. PSI indices are presented in Supplemental

291   Table S4.

292   Supplemental Table S5 presents normalized PSI.

293   Normalized PSI index shows that postures are highly similar to each other in synergy space. This

294   is expected, as we have performed analysis for a single posture with different trials. Note however

295   that, even for the same posture, across different trials, PSI is not expected to reach the theoretical

296   maximum of 1. This is because, although functionally it is the same posture, the exact joint angles

297   may vary and hence PSI may not reach the theoretical maximum. However, we expect the PSI to

298   be higher across trials of the same posture when compared to PSI across postures.

299 This example shows that our method works well both on real experimental and synthetic data in
300 synergy space. Finding PSI for the set of hand postures will give a quantification measure from
301 the perspective of overlap in synergy space.

302 **Representative postures**

303 For finding representative postures, we further used PSI for identifying the most significant set of
304 postures ("Eigen postures"). We added column-wise PSIs – this represents the overall similarity
305 that a posture has with all other postures. We then added row-wise to determine the total PSI value.
306 Using these values, we developed a relative PSI index presented in the following equation (7).

$$Relative\ PSI_c = \frac{\sum_{i=1}^{100} PSI_{c,i}}{\sum_{i,j=1}^{100} PSI_{i,j}} \tag{7}$$

307

308 In equation (7), C is column-wise PSI value.

309 Further, we sorted the relative PSI in ascending order. The leftmost element represents the posture
310 with the lowest similarity and as we move from left to right relative PSI index increases. The
311 rightmost element has maximum relative PSI. Cumulative relative PSIs were computed by
312 summing up the sorted relative PSI curve. We computed the first derivative of cumulative relative
313 PSI and determined its peak. Postures on the right-hand side of the peak value are representative
314 postures. We call these postures as representative postures, since they help in deriving other
315 postures based on kinematic synergies. The representative postures are more associated with many
316 other postures from the synergy point of view.

317 The peak of the derivative of relative PSI is not expected to happen at the same posture number
318 across participants. Also, it is not necessary for the same postures to lie on the right side of this
319 peak. In other words, it is not theoretically necessary for the same postures to be representative in
320 all participants. The most common postures found among representative postures in different
321 participants are presented in the Results section.

322 **Results**

323   **Kinematic synergy using linear method**

324   (Figure 5)

325   As shown in Figure 5, DIP vs PIP joint angle shows that there is a strong linear relationship

326   (r^2=0.997) between the joint angles of DIP and PIP. These results are in line with previous studies

327   (Cerveri et al., 2007; Cobos et al., 2008; Cobos et al., 2010; Bullock et al., 2012).

328   We performed PCA by centering data and using Singular Value Decomposition (SVD) algorithm.

329   Results were averaged across participants and presented in Figure 6. From Figure 6 we observe

330   that in synergy space 1st PC explains approximately 40% of total variance and nearly first 5 PCs

331   explained 84% of total variance in data. First 10 PCs explain approximately 95% of the total

332   variance.

333   (Figure 6)

334   Static joint angles were reconstructed using 1st N PCs (i.e. Synergies) where N varies from 2 to

335   21. As expected, joint angle reconstruction error reduces as more number of kinematic synergies

336   are involved. Joint angle reconstruction error was computed across all joints, across twelve

337   participants as shown in Figure 7. The shaded region represents standard error of mean across

338   participants.

339   (Figure 7)

340   From the result in Figure 7, we find that the error in joint angle reconstruction is higher when

341   considering few synergy components. The experiment involves not only activities of daily living

342   but also ASL and aesthetic (Bharatanatyam) postures.

343   The *posture similarity index* analysis was run for all participants separately. For analysis, one out

344   of five trials was selected randomly for all the 100 postures. PSI matrix (100x100) gives the

345   similarity between any two postures in the dataset. We have presented the PSI matrix for a single

346   participant in Figure 8.

347   (Figure 8)

348   Based on the PSI matrix shown in Figure 8, posture 11 was selected and compared with the rest of

349   the postures for illustration purpose. In Figure 9, we have presented postures in the descending

350   order of posture similarity index for top five PSI values.

351   (Figure 9)

352   Based on PSI value, posture 15 is most similar to posture 11. Postures 37, 58 and 3 have lower

353   similarity with posture 11. Posture 11 and 15 share common features such as the posture of the

354   thumb. However, the postures of other fingers are different. The high similarity between postures

355   11 and 15 means that there is more significant overlap between these postures. Posture 37 which

356   shares a similar thumb position as posture 11 has large PSI value. In posture 58, index and middle

357   fingers are straight, similar to posture 11, which causes more substantial similarity; but ring and

358   little fingers are flexed. Posture 3 shares common features such as the abduction of middle, ring,

359   and little finger which results in high PSI value. For each participant, the PSI matrix is unique.

360   **Representative postures**

361   For finding representative postures, relative PSI values were computed by summing all the PSI

362   values for a posture and finding the ratio with total PSI value of a matrix for each posture

363   separately, as shown in Figure 10 (A). Postures were rearranged in ascending order based on

364   relative PSI index and the first derivative of relative PSI was determined as shown in Figure 10

365   (B).

366   (Figure 10)

367   The peak value was measured for each participant. For comparison, we used the smallest peak

368   across participants as the peak. Since the representative postures are not expected to be the same

369   across participants, we present the most common postures in Figure 11 (We have presented only

370   those postures found across at least 7 participants).

371   (Figure 11)

372   **Statistical analysis**

373 Many representative postures in the dataset included more "special" postures rather than common

374 postures. However, the number of "special" postures used in the experiment was comparatively

375 more than common postures. To rule out the possibility that the representative postures had more

376 "special" postures purely because they were larger in number in the overall dataset, we normalized

377 the number of representative postures by the respective number of postures present in the actual

378 dataset separately for "special" and common postures. The paired t-test showed that the number

379 of common postures is significantly lesser than the number of special postures in a set of

380 representative postures. Further, we performed one-way repeated measures ANOVA, with the type

381 of posture (i.e. common Vs special) as a factor on the number of postures present in the

382 representative postures. We found that the number of special postures is significantly higher ($F_{(1,11)}$

383 = 39.99; $p<0.001$) than the number of common postures (Mean ± standard error, common Vs

384 "special": 16.91 ± 0.96 Vs 29.75 ± 0.98). These findings revealed that for the given dataset more

385 number of "special" postures are represented in synergy subspace in comparison with common

386 postures. We illustrate these results in Figure 12.

387   (Figure 12)

388 **Discussion**

389 This article showcases a novel approach for comparing hand postures using synergies (PCA). Our

390 method uses a ratio of variances in Eigen directions generated by PCA for comparison of two static

391 hand postures. Posture similarity index (PSI) is a measure of similarity of two postures in the

392 synergy space. Further, we used this index to identify representative postures from a large pool of

393 various postures including common postures (activities of daily living   ADL) and "special"

394 postures. Our approach which involved combining the original structure of hand postures allows

395 the relative comparison of the overlap in synergy space between two postures. We use this index

396 to identify a set of representative postures. We discuss the implications of our findings in the

397 following sections.

398

399 **Kinematic synergies during performance of a dynamic task**

400 In the literature, several studies have documented evidence for synergies in constrained and

401 unconstrained exploration tasks. These have involved environmental constraint exploration,

402   unconstrained exploration, and grasping of real and imaginary objects (Santello et al 1998). Thakur

403   et al., (2008) documented the existence of task-independent synergy components across several

404   tasks, while the participants were blindfolded and were allowed relatively free haptic exploration

405   of several real-life objects. They also found that some of these synergies are similar across several

406   participants. In more recent studies, (Della Santina et al., 2017, Eppner et al., 2015) constrained

407   exploration has been used to document the existence of kinematic synergies. In our study, we have

408   used one hundred different postures, comprising of relatively new ("special postures", including

409   ASL, Bharatanatyam postures) and familiar ("common", daily life postures) postures in addition

410   to some real-life object grasping postures. Our results from the synergy perspective are in-line with

411   previous studies (Santello et al 1998). However, it must be noted that in our study we have

412   analyzed static posture (70 data samples per trial per posture), but not the actual movement

413   (kinematics involving exploration, pre-shaping). Our goal here was to develop an index that

414   captured the similarity of postures in the synergy space. Hence, we considered each posture and

415   compared with other postures within the synergy (PCA) space. Hence, our "representative

416   postures" are "representative" among the 100 postures considered, but not a combination of several

417   postures as in synergies. Since we used a relatively large number of postures, we believe that our

418   representative postures could also be "representative" in a real-life sense, although this is just a

419   speculation. This is because the human hand can perform a myriad number of postures and we

420   have only considered 100 of those postures.

421   **Use of human hand synergies in the development of robotic hands**

422   One application of human hand synergies involves the development of dexterous robots and

423   prosthetic devices. Several groups have developed and documented synergy based robotic hands

424   (Ciocarlie & Allen 2009, Brown & Asada 2007, Fani et al., 2016). It is unclear, however, whether

425   anthropomorphism is the best possible strategy for using synergies in building better robotic hands

426   (Santello et al. 2016). However, in cases involving an interaction of a human with robots,

427   anthropomorphism is arguably a desirable feature. It has also been suggested that a mechanism

428   similar to motor synergies in hand may underlie the function of mirror neurons (D'Ausilio et al

429   2015). Anthropomorphism index (AI) has been used for comparing human hand posture with

430   artificial hand using a projection of multi-dimensional posture into two-dimensional nonlinear

431   subspace (Feix et al., 2013). The method uses a comparison on a cell to cell basis in two-

432   dimensional space. However, this method assumes that we can reconstruct the actual posture from

433   two-dimensional nonlinear subspace. In our study, we developed the PSI, which compares two

434   postures performed by humans in the synergy space. Here we project the postures to the synergy

435   space to perform the comparison. PSI considers the variance in all directions which assure accurate

436   hand posture reconstruction. A significant value of PSI represents high similarity between two

437   postures and gives an indication of more substantial overlap in synergy space between these

438   postures. PSI values are not always intuitive due to the abundance in the motor system.

439   **Representative postures and synergies – Possible neural mechanisms**

440   Synergies are neuronal structural units which the central nervous system uses as the basis for

441   generating any new posture (Santello et al., 1998; Mason et al., 2001; Leo et al., 2016). In our

442   study, we use representative postures. These are individual elements that are most represented

443   through multiple postural synergies, not elements of synergy. One recent study has suggested that

444   a small number of muscle synergies may underlie a large number of grasps (Scano et al., 2018).

445   Our results, in the joint angle space, agrees with these results; further, we present the common

446   postures across participants. Several studies have documented evidence for synergistic movement

447   of fingers through neural stimulating (Gentner and Classen, 2006; Gentner et al., 2010) in primary

448   motor cortex, similar to a study that involves grasping of an imagined object (Santello et al., 1998;

449   Leo et al., 2016). These findings provide strong support to the notion of a synergistic representation

450   in brain areas. We believe that our representative postures are those that seek equal action manifold

451   in comparison to our large set of postures. Our finding also suggests that significantly large number

452   of "special" postures are part of representative postures rather than common postures. We believe

453   that this may be because a smaller number of synergies can capture overlearned tasks. But such

454   smaller number of synergies may not be able to capture the tremendous behavioral flexibility in

455   the human system (Gentner et al., 2010). Hence, common postures occupy lesser space and are

456   more concentrated whereas "special" postures are spread across synergy space. Our method

457   captures this effect reasonably well.

458   **Concluding comments**

459   In this study, we have defined, developed and demonstrated the use of a synergy based posture

460   comparison index, PSI. It is also useful to classify postures as "representative" or otherwise. A

461   limitation of the current approach is that comparison between two hand postures depends on the

462 complexity of hand model. Our hand model consists of 21 DoF model, which does not account for

463 the palm arch and wrist joints. PSI may give more insightful results for a complex model involving

464 multiple degrees of freedom. Distribution of data may provide more hidden information about

465 hand postures and will be able to produce more accurate results.

466 **References**

467 1. Brown CY., Asada HH. 2007. Inter-finger coordination and postural synergies in robot hands via

468 mechanical implementation of principal components analysis. In: *Intelligent Robots and Systems,*

469 *2007. IROS 2007. IEEE/RSJ International Conference on*. IEEE, 2877–2882.

470 2. Bullock IM., Borràs J., Dollar AM. 2012. Assessing assumptions in kinematic hand models: a

471 review. In: *Biomedical Robotics and Biomechatronics (BioRob), 2012 4th IEEE RAS & EMBS*

472 *International Conference on*. IEEE, 139–146.

473 3. Cavallo A., Koul A., Ansuini C., Capozzi F., Becchio C. 2016. Decoding intentions from

474 movement kinematics. *Scientific Reports* 6:37036.

475 4. Cerveri P., De Momi E., Lopomo N., Baud-Bovy G., Barros RML., Ferrigno G. 2007. Finger

476 kinematic modeling and real-time hand motion estimation. *Annals of biomedical engineering*

477 35:1989–2002.

478 5. Ciocarlie MT., Allen PK. 2009. Hand posture subspaces for dexterous robotic grasping. *The*

479 *International Journal of Robotics Research* 28:851–867.

480 6. Cobos S., Ferre M., Ángel Sánchez-Urán M., Ortego J., Aracil R. 2010. Human hand descriptions

481 and gesture recognition for object manipulation. *Computer methods in biomechanics and*

482 *biomedical engineering* 13:305–317.

483 7. Cobos S., Ferre M., Uran MS., Ortego J., Pena C. 2008. Efficient human hand kinematics for

484 manipulation tasks. In: *Intelligent Robots and Systems, 2008. IROS 2008. IEEE/RSJ International*

485 *Conference on*. IEEE, 2246–2251.

486 8. D'Ausilio A., Bartoli E., Maffongelli L. 2015. Grasping synergies: a motor-control approach to

487 the mirror neuron mechanism. *Physics of life reviews* 12:91–103.

9. Della Santina C., Bianchi M., Averta G., Ciotti S., Arapi V., Fani S., Battaglia E., Catalano MG., Santello M., Bicchi A. 2017. Postural Hand Synergies during Environmental Constraint Exploitation. Frontiers in Neurorobotics 11. DOI: 10.3389/fnbot.2017.00041

10. Deuschl G., Raethjen J., Lindemann M., Krack P. 2001. The pathophysiology of tremor. *Muscle & nerve* 24:716–735.

11. Eppner C., Deimel R., Álvarez-Ruiz J., Maertens M., Brock O. 2015. Exploitation of environmental constraints in human and robotic grasping. The International Journal of Robotics Research 34:1021–1038.

12. Fahn S., Jankovic J., Hallett M. 2011. *Principles and Practice of Movement Disorders E-Book.* Elsevier Health Sciences.

13. Fani S., Bianchi M., Jain S., Pimenta Neto JS., Boege S., Grioli G., Bicchi A., Santello M. 2016. Assessment of myoelectric controller performance and kinematic behavior of a novel soft synergy-inspired robotic hand for prosthetic applications. *Frontiers in neurorobotics* 10:11.

14. Feix T., Romero J., Ek CH., Schmiedmayer H-B., Kragic D. 2013. A metric for comparing the anthropomorphic motion capability of artificial hands. *IEEE transactions on robotics* 29:82–93.

15. Gentner R., Classen J. 2006. Modular organization of finger movements by the human central nervous system. *Neuron* 52:731–742.

16. Gentner R., Gorges S., Weise D., aufm Kampe K., Buttmann M., Classen J. 2010. Encoding of motor skill in the corticomuscular system of musicians. *Current Biology* 20:1869–1874.

17. Hoyet L., Ryall K., McDonnell R., O'Sullivan C. 2012. Sleight of hand: perception of finger motion from reduced marker sets. In: *Proceedings of the ACM SIGGRAPH Symposium on Interactive 3D Graphics and Games*. ACM, 79–86.

18. Jazar, R. N. (2010). Theory of applied robotics: kinematics, dynamics, and control. Springer Science & Business Media.

19. Jerde TE., Soechting JF., Flanders M. 2003a. Biological constraints simplify the recognition of hand shapes. *IEEE transactions on biomedical engineering* 50:265–269.

514   20. Leo A., Handjaras G., Bianchi M., Marino H., Gabiccini M., Guidi A., Scilingo EP., Pietrini P.,

515   Bicchi A., Santello M., Ricciardi E. 2016. A synergy-based hand control is encoded in human

516   motor cortical areas. *eLife* 5:e13420. DOI: 10.7554/eLife.13420.

517   21. Mason CR., Gomez JE., Ebner TJ. 2001. Hand synergies during reach-to-grasp. *Journal of*

518   *Neurophysiology* 86:2896–2910.

519   22. McAuley JH., Marsden CD. 2000. Physiological and pathological tremors and rhythmic central

520   motor control. *Brain* 123:1545–1567.

521   23. Rezzoug, N., and Gorce, P. (2008). Prediction of fingers posture using artificial neural networks.

522   Journal of Biomechanics, 41(12), 2743–2749.

523   24. Roweis ST., Saul LK. 2000. Nonlinear dimensionality reduction by locally linear embedding.

524   *science* 290:2323–2326.

525   25. Santello M., Bianchi M., Gabiccini M., Ricciardi E., Salvietti G., Prattichizzo D., Ernst M.,

526   Moscatelli A., Jörntell H., Kappers AM. 2016. Hand synergies: integration of robotics and

527   neuroscience for understanding the control of biological and artificial hands. *Physics of life*

528   *reviews* 17:1–23.

529   26. Santello M., Flanders M., Soechting JF. 1998. Postural hand synergies for tool use. *Journal of*

530   *Neuroscience* 18:10105–10115.

531   27. Scano A., Chiavenna A., Molinari Tosatti L., Müller H., Atzori M. 2018. Muscle Synergy

532   Analysis of a Hand-Grasp Dataset: A Limited Subset of Motor Modules May Underlie a Large

533   Variety of Grasps. *Frontiers in Neurorobotics* 12. DOI: 10.3389/fnbot.2018.00057.

534   28. Thakur PH., Bastian AJ., Hsiao SS. 2008. Multidigit Movement Synergies of the Human Hand in

535   an Unconstrained Haptic Exploration Task. Journal of Neuroscience 28:1271–1281.

536   29. Todorov E., Ghahramani Z. 2004. Analysis of the synergies underlying complex hand

537   manipulation. In: *Engineering in Medicine and Biology Society, 2004. IEMBS'04. 26th Annual*

538   *International Conference of the IEEE*. IEEE, 4637–4640.

539   30. Todorov E., Jordan MI. 2002. Optimal feedback control as a theory of motor coordination.

540   *Nature neuroscience* 5:1226.

541   31. Wheatland N., Jörg S., Zordan V. 2013. Automatic hand-over animation using principle

542   component analysis. In: *Proceedings of Motion on Games*. ACM, 197–202.

543   32. Wu G., van der Helm FCT., Veeger HEJD., Makhsous M., Van Roy P., Anglin C., Nagels J.,

544   Karduna AR., McQuade K., Wang X., Werner FW., Buchholz B., International Society of

545   Biomechanics 2005. ISB recommendation on definitions of joint coordinate systems of various

546   joints for the reporting of human joint motion--Part II: shoulder, elbow, wrist and hand. *Journal*

547   *of Biomechanics* 38:981–992.

548   33. Zatsiorsky, V. M. (1998). Kinematics of human motion, Human Kinetics. Urbana Champaign.

549

Figure 1

(a) Sensor placement location on hand. (b) Kinematic hand model consisting of 21 DoFs.

(a) Fifteen sensors are placed on digits and one reference sensor is placed near wrist. (b) DIP and PIP joints corresponds to 1 DOF; MCP joint corresponds to 2 DOFs; for thumb CMC joint corresponds to 3 DOFs. All photographs by Varadhan SKM. Hand model: Nayan Bhatt.
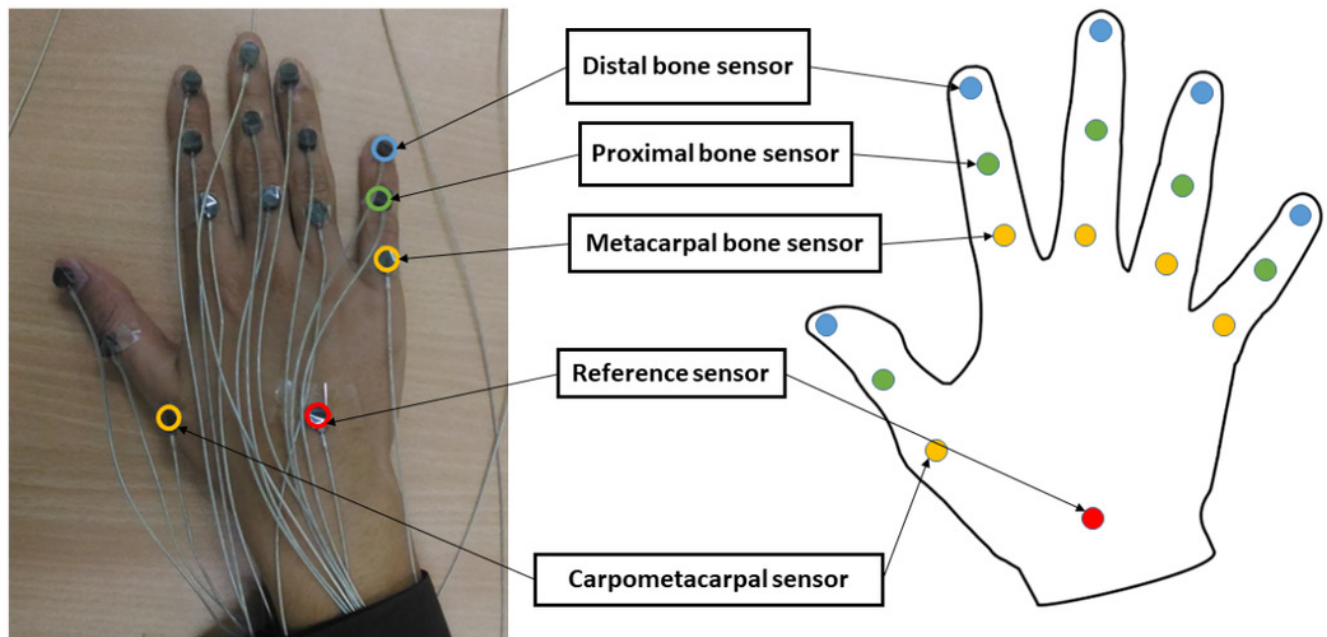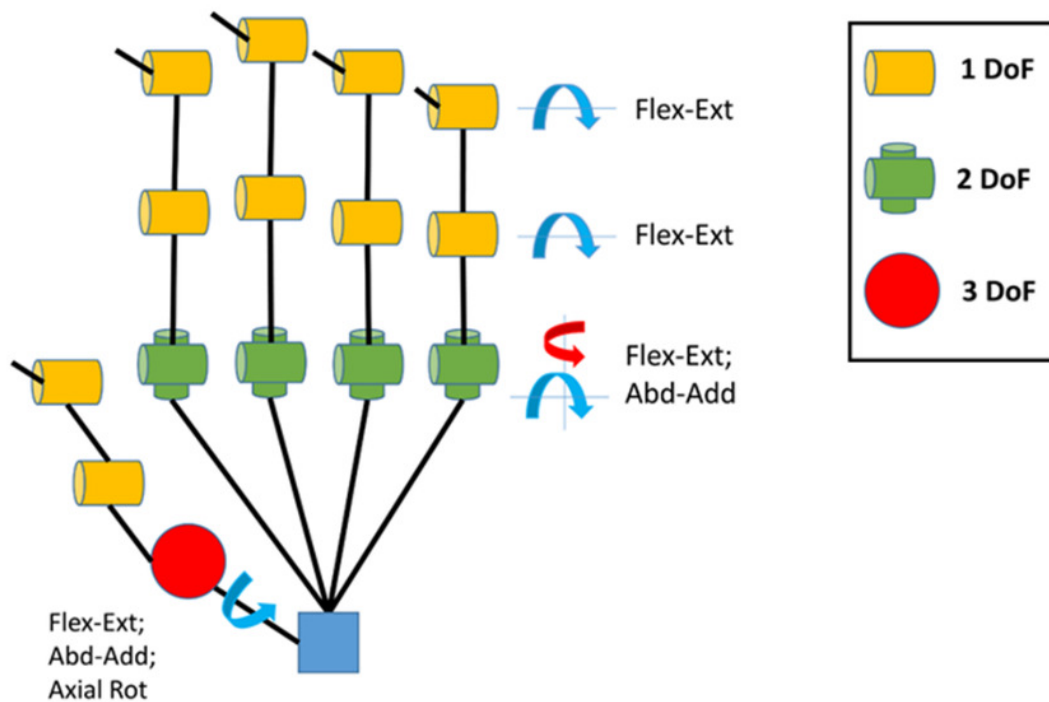
Figure 2

Experimental setup.

Participants were seated in a height-adjustable chair. Placement of the transmitter was based on biomechanical standards (Wu et al., 2005). The computer screen was placed approximately 1 m away from the participant. Image of posture was shown to the participant on the screen. Participants were asked to perform posture which is shown on the screen starting from the base posture.
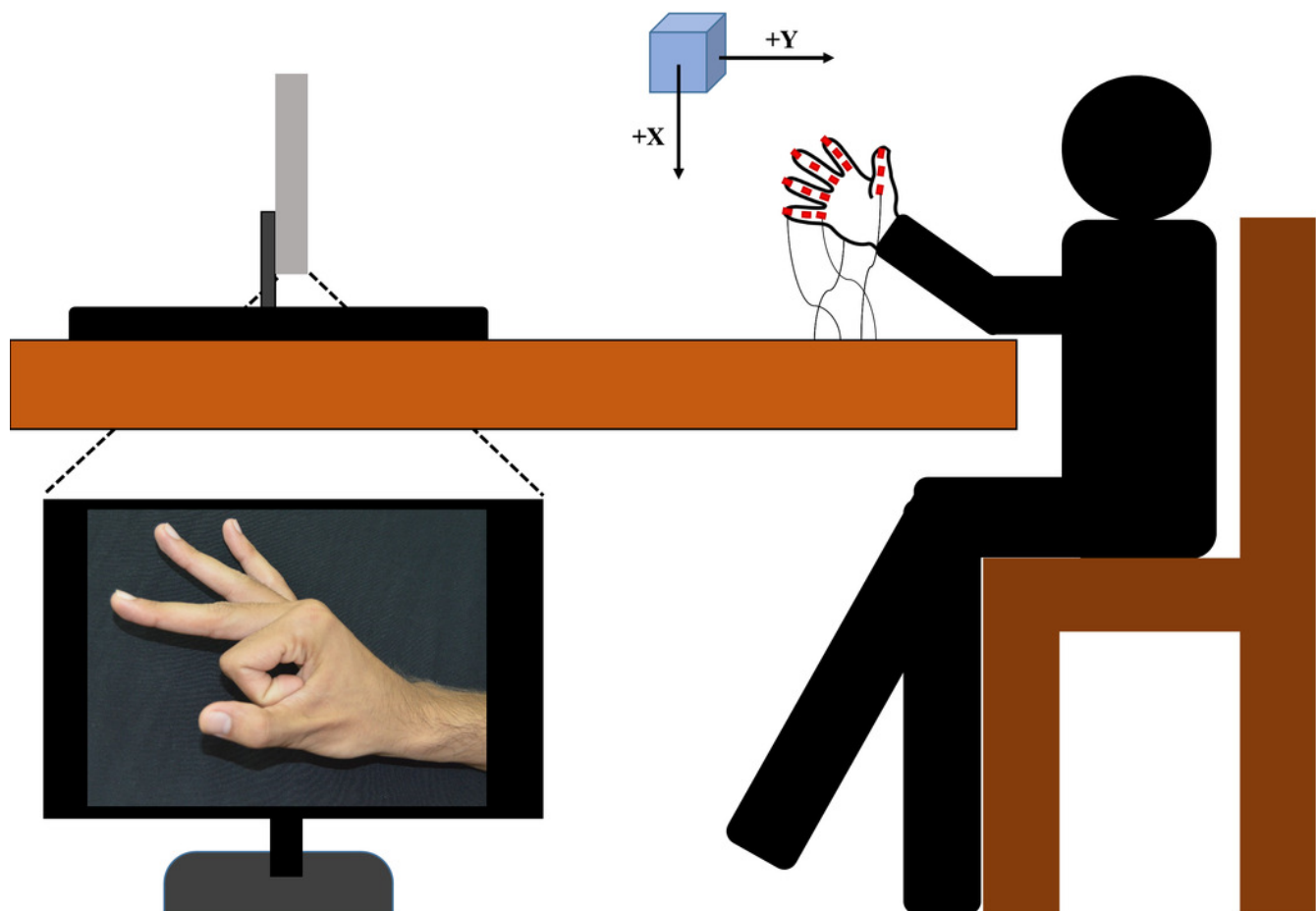
Figure 3

(a) Simulated postures in 3D space. (b) Variance in the synergy space for synthetic dataset.

(a) Posture 1 and posture 2 have same covariance matrix but different mean values. Mean of posture 3 is closer to posture 1, which means there is an overlap between posture 1 and 3. Structure of posture 1 and 3 are different. (b) Synergy 1 represents highest variance (i.e. ~77.8%), Synergy 2 explains (~15.8%) variance, and Synergy 3 explains (~6.7%) variance.
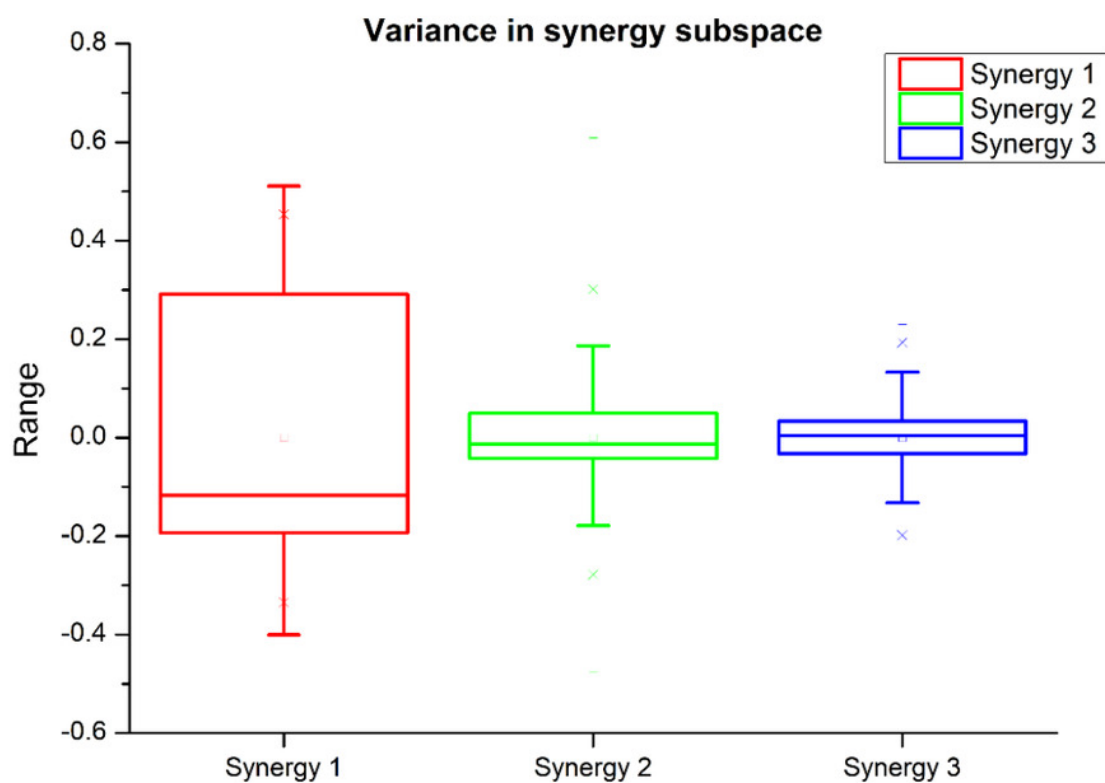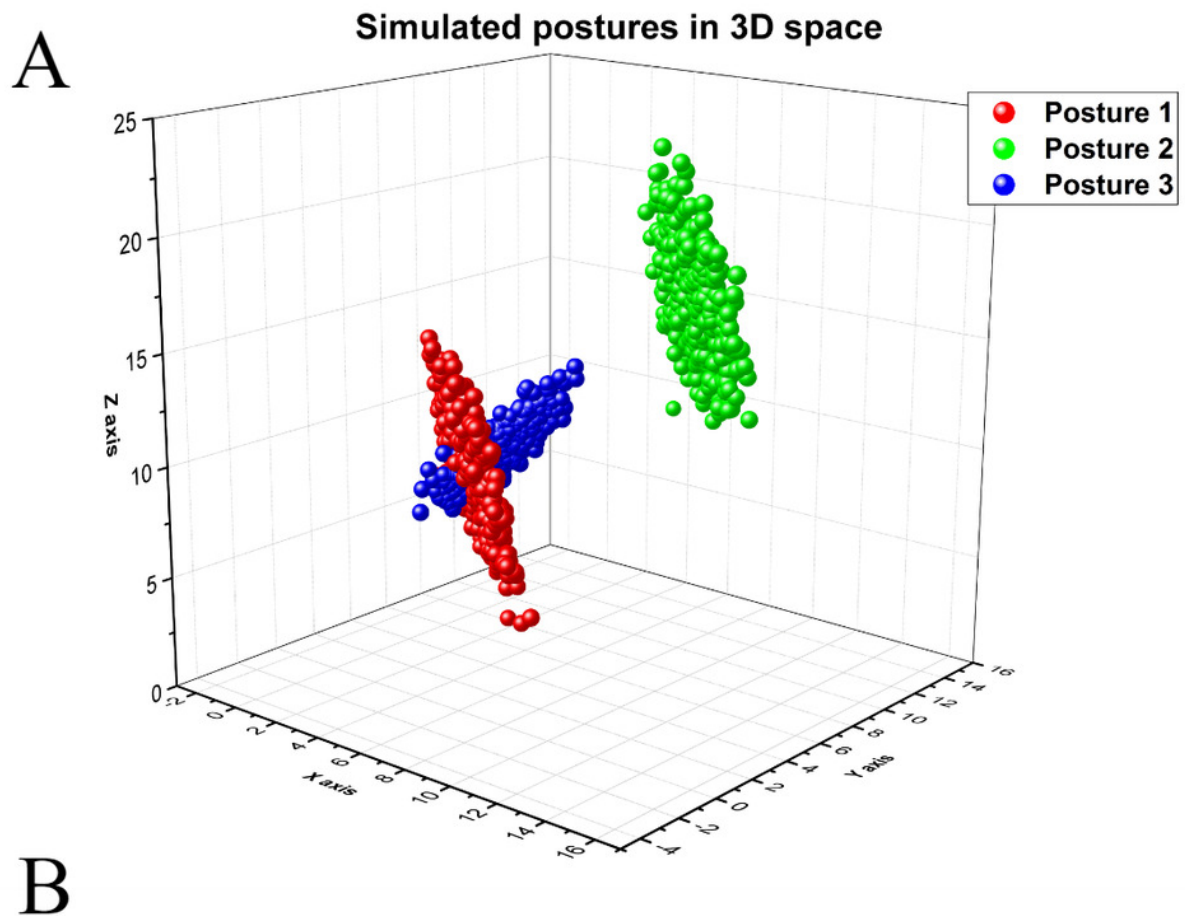
Figure 4

Scree plot for actual postures with three trials

PC1 explains approximately 63.6% of variance, PC2 and PC3 explains nearly 23% and 9% of variance respectively.
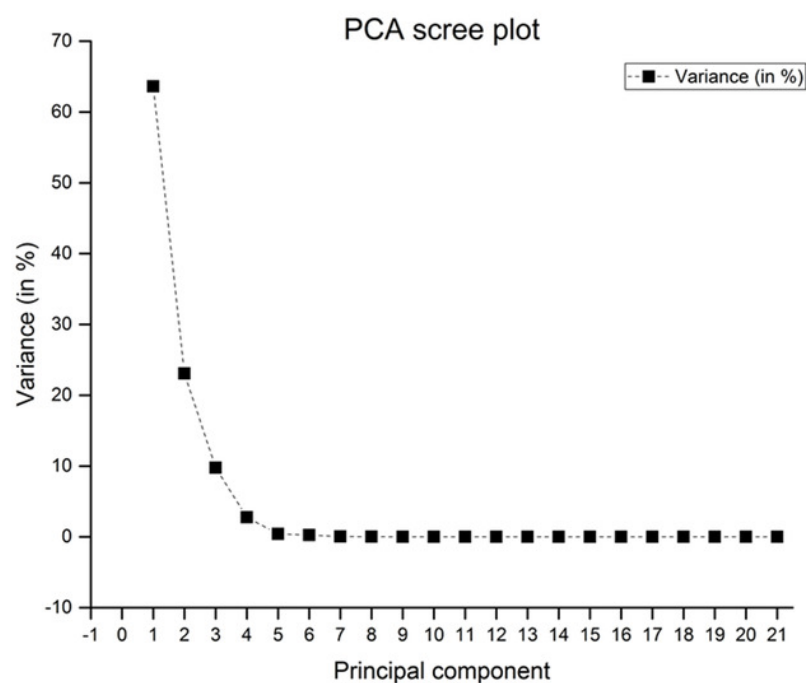
Figure 5

Mean value between DIP-PIP joints for a single trial across participants

Joint angle relation between distal interphalangeal (DIP) and Proximal interphalangeal (PIP) joints.
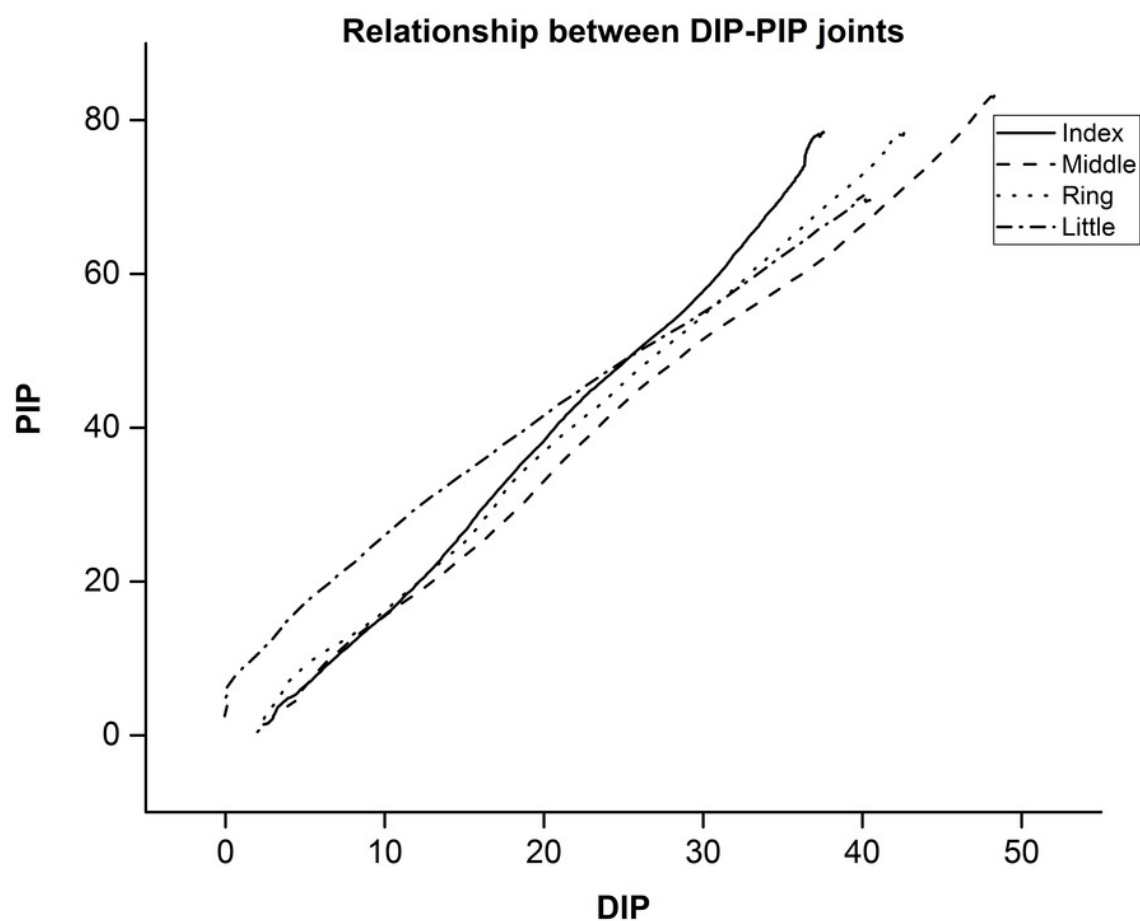
Figure 6

PCA variance explained by a principal component

1st PC explains nearly 40% of variance and 2nd PC explains nearly 20% of variance, error bar represents standard error of mean across participants.
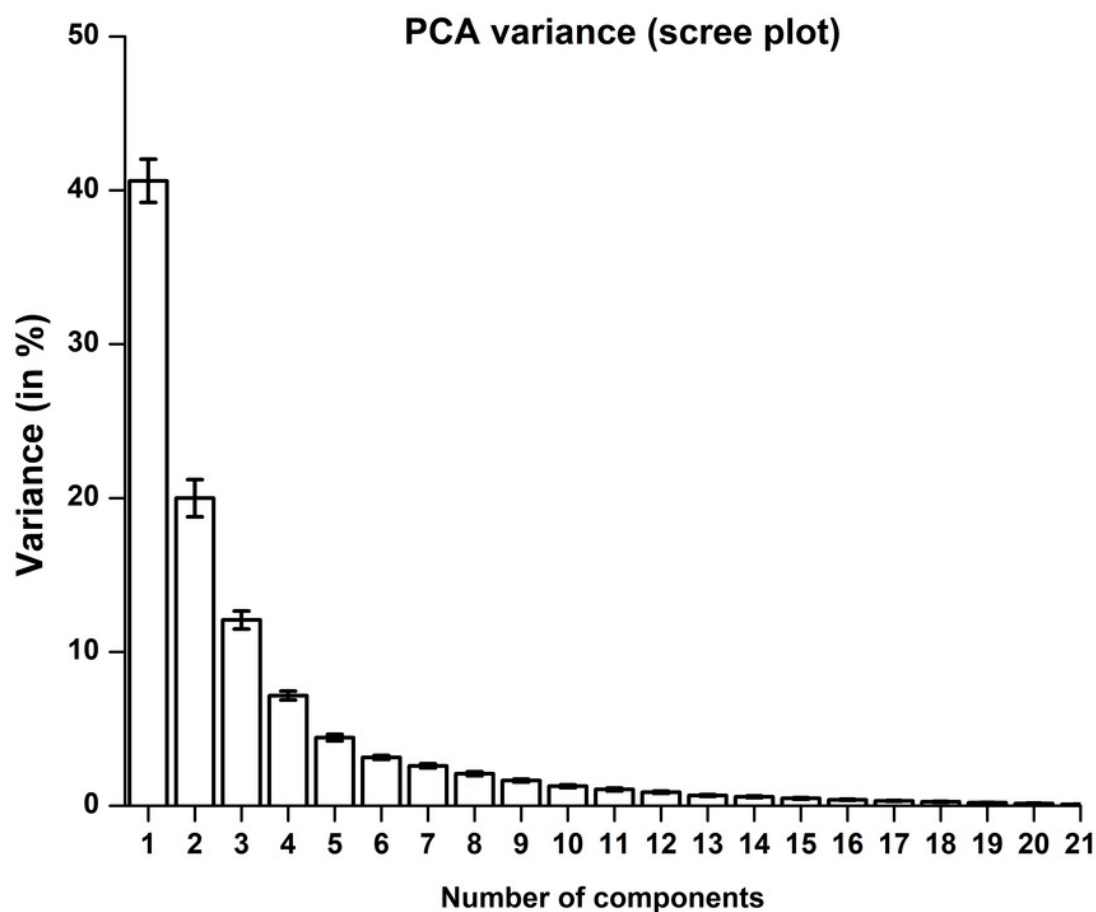
Figure 7

Joint angle reconstruction error.

Mean squared error across postures were plotted against number of synergy components counted. Joint angle reconstruction error reduces as more number of synergy components were introduced.
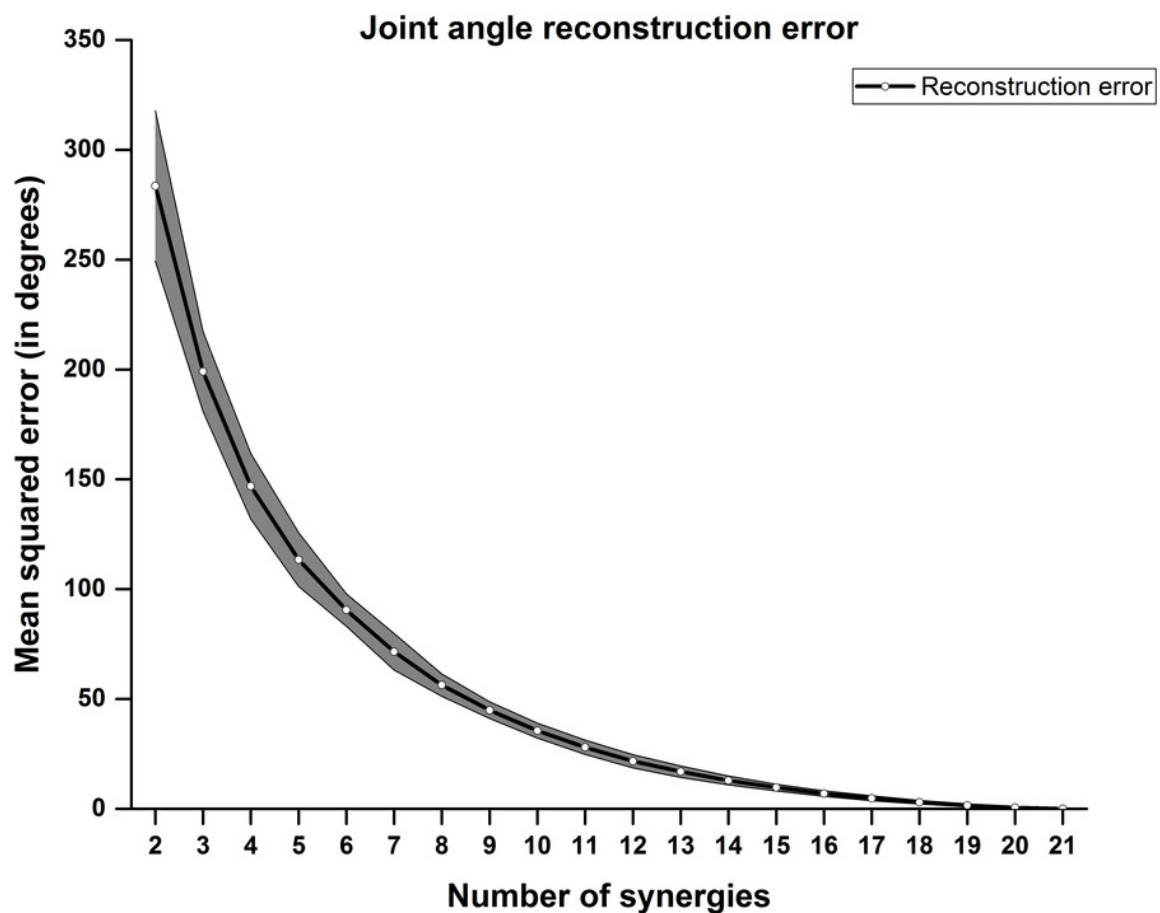
Figure 8

Colour map representation of PSI matrix.

Dark red colour represents very high similarity between postures in synergy space where as blue colour represents low similarity between postures.
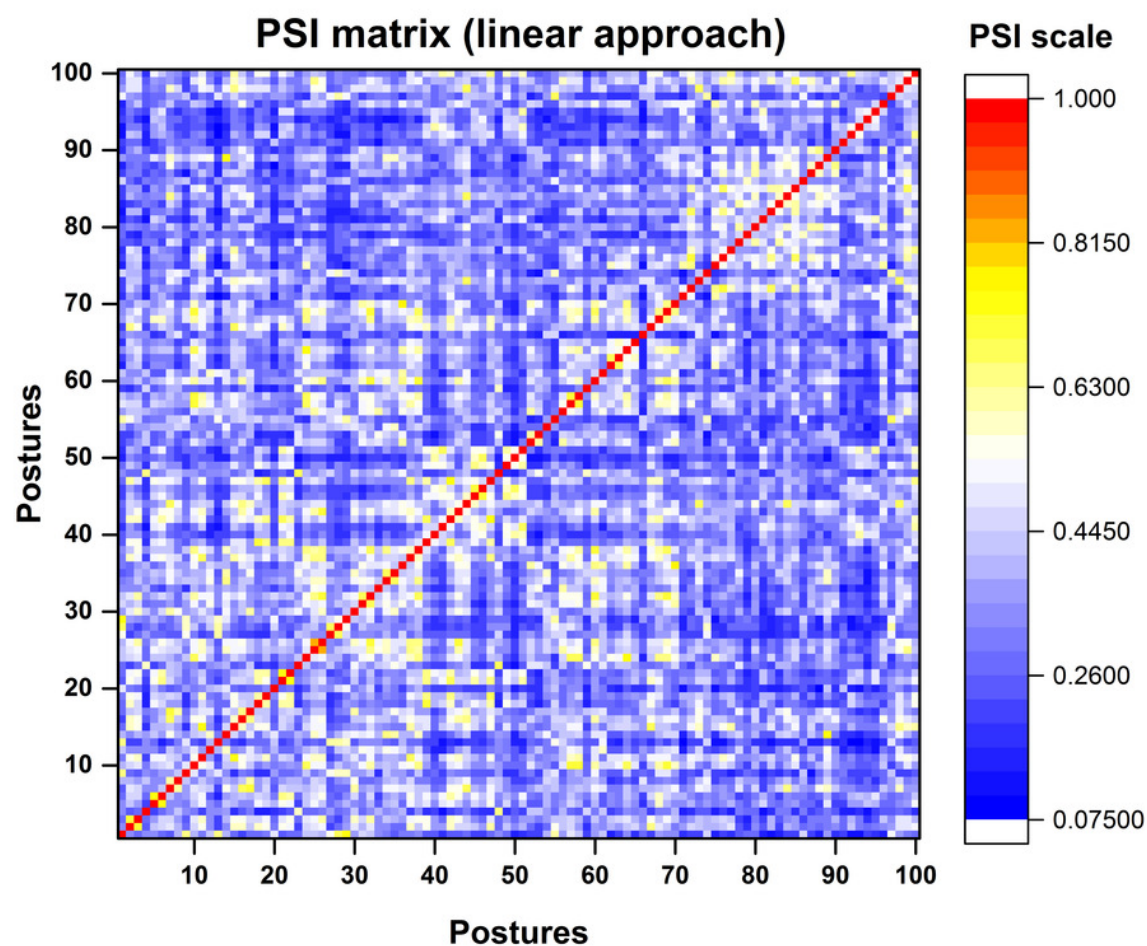
Figure 9

Top five Postures based on PSI values

All photographs by Varadhan SKM. Hand model: Nayan Bhatt.
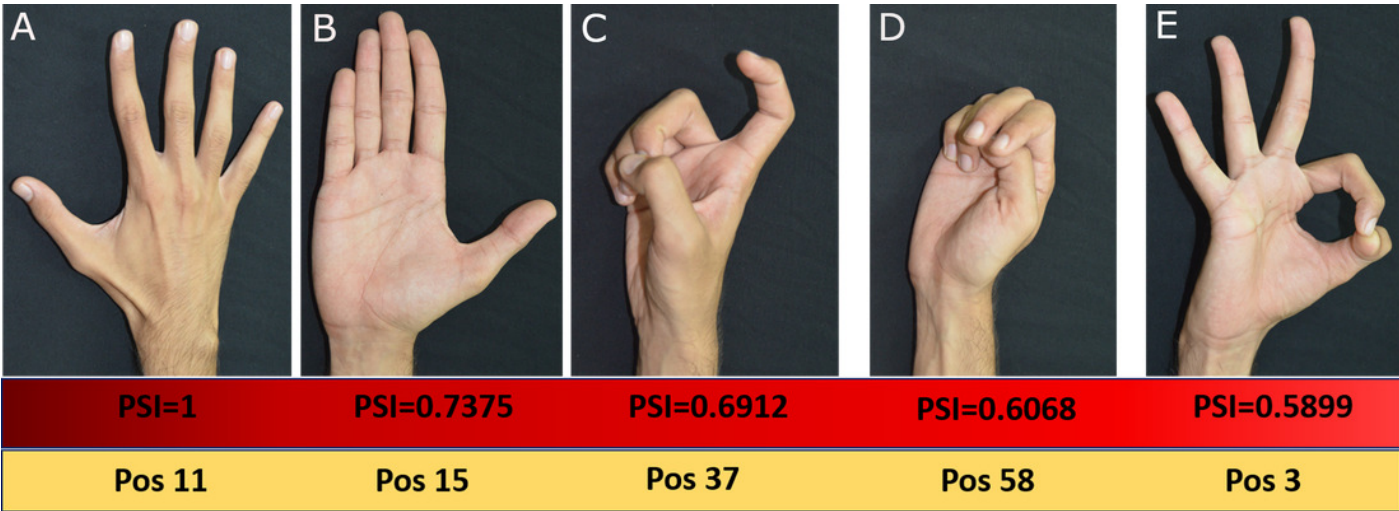
Figure 10

(a) Cumulative relative PSI index. (b) First derivative of relative PSI index for all participants.
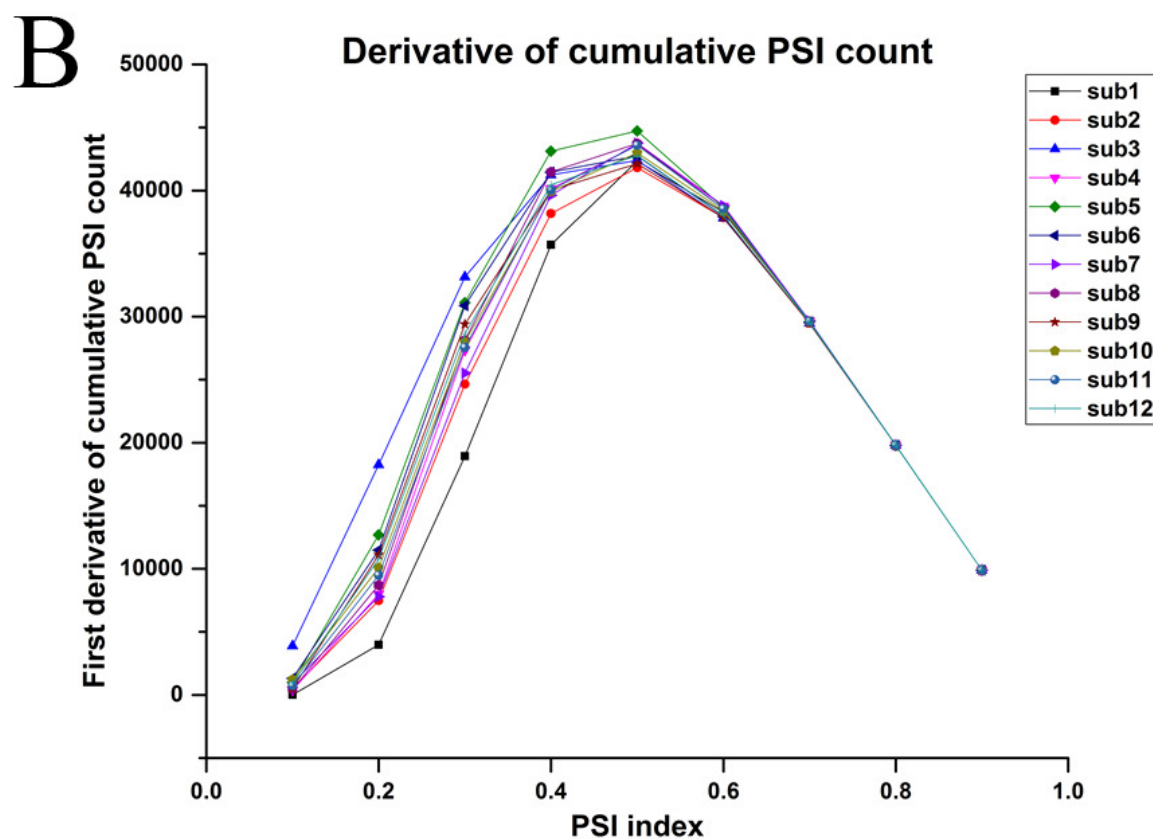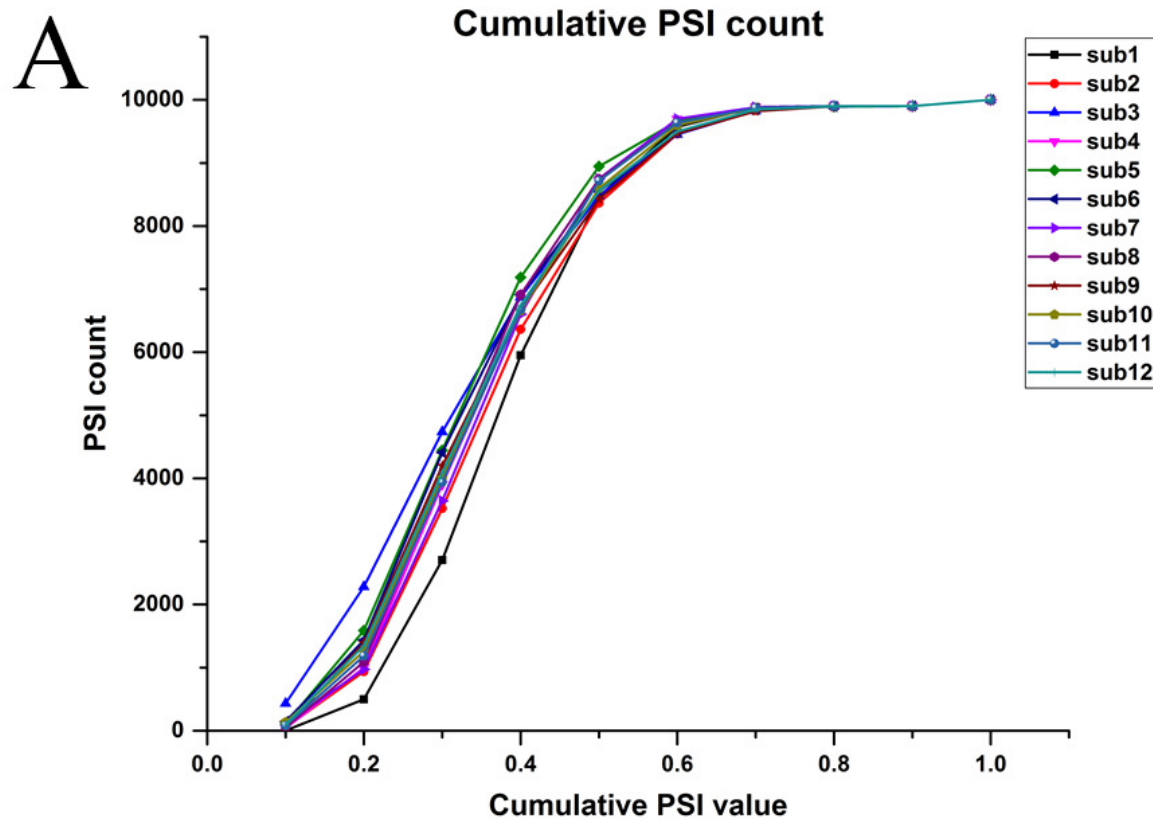
Figure 11

Set of representative postures present in most participants

(a) Most common representative posture - present in all 12 participants. (b) Common postures observed in 11 participants. (c) Common postures observed in 10 participants. (d) Common postures observed in 9 participants. (e) Common postures observed in 8 participants. (f) Common postures observed in 7 participants.
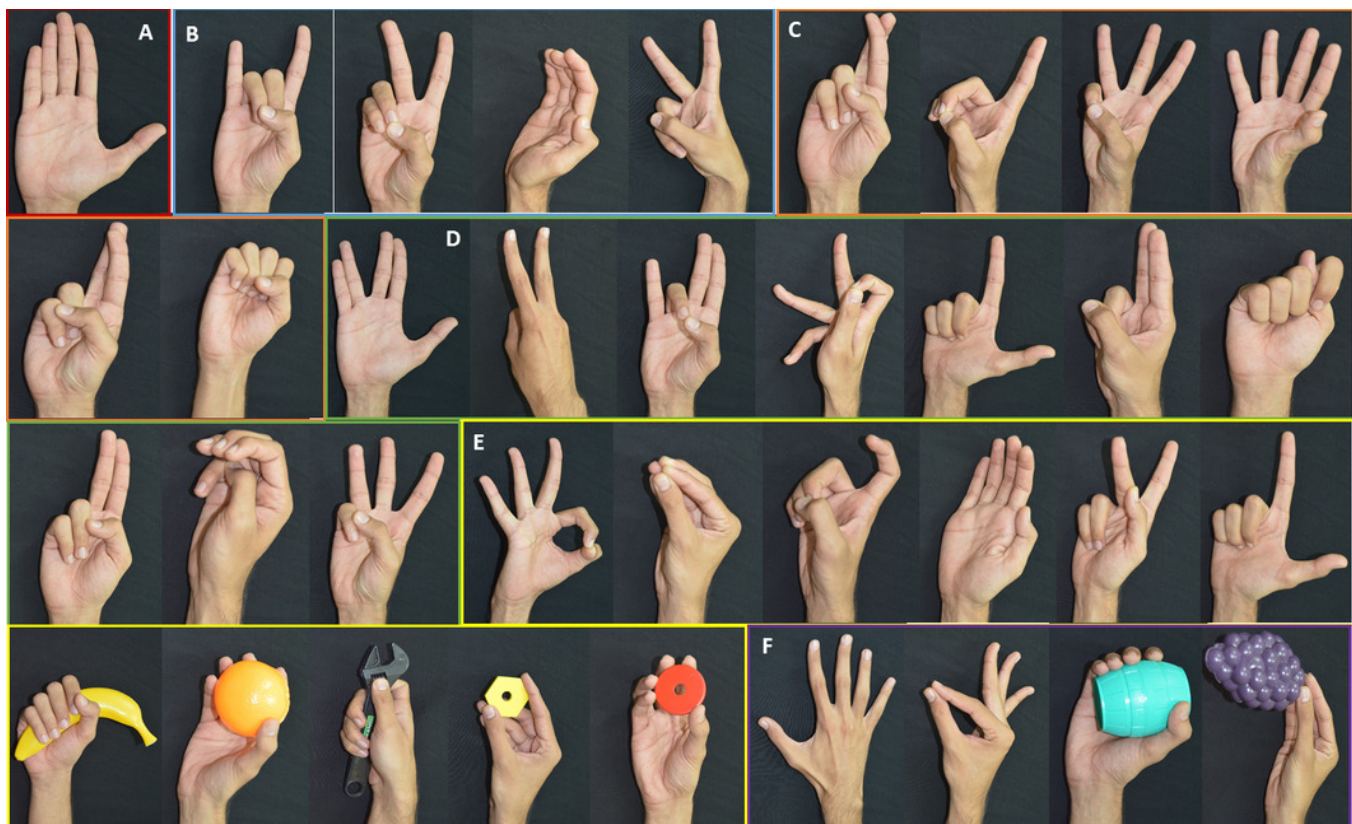
Figure 12

Task dependent representative posture count.

Number of representative special postures are significantly large in synergy space in comparison with common postures.